DIFFRACTION AND EXCLUSIVE PROCESSES AT HERA[a]

J. OLSSON (on behalf of the H1 and ZEUS collaborations)
DESY, Notkestraße 85, 22603 Hamburg, Germany
E-mail: jan.olsson @ desy.de

A review is given of selected recent results from the H1 and ZEUS experiments at the HERA ep collider. The results cover exclusive elastic and proton-dissociative diffractive vector meson production, and are obtained in wide ranges of $W_{\gamma p}, Q^2, |t|$ and vector meson mass M_V. A comparison is made with recent theoretical calculations and it is shown that perturbative QCD models are successful in describing the processes when the involved scales have large values.

1 Introduction

The large data samples collected during the years 1994-97 by the H1 and ZEUS experiments at the ep collider HERA at DESY are the basis for the results, which are presented in this report. The beam energies in these years were 27.5 GeV(e^+) and 820 GeV(p), yielding a center of mass (CM) energy of $\sqrt{s} = 300$ GeV.
The simplest exclusive production process in diffractive ep scattering is the process

$$ep \to\ eVp, \quad \text{where } V \text{ is a vector meson } \ \rho^\circ, \omega, \phi, \rho', J/\Psi, \Psi', \Upsilon.$$

These processes have been studied since a long time at lower energies, in fixed target experiments. Although a simple reaction, the exclusive vector meson production has served as a rich source of information on the nature of the diffractive process. The HERA colliding beam experiments greatly extend the accessible range both of the center of mass energy and of the various scales which influence the reaction. Thus, with the data from HERA detailed studies of the diffractive vector meson production are made possible, both in the soft, low-energy regime already explored by the fixed target experiments, and in the new regimes, where the involved scales reach large values and perturbative QCD (pQCD) can be applied.
Although the bulk of the results cover the elastic vector meson production, i.e. those reactions where the outgoing proton stays intact, some results will also be described, in which the proton dissociates into a low-mass hadronic system.

[a]Talk given at the Intern. Conference on Elastic and Diffractive Scattering, 27.6-2.7.1999, Protvino, Russia (EDS 99, VIIIth “Blois Workshop”)

The diagram of Fig.1 illustrates that HERA in fact can be viewed as a collider of virtual photons γ^* with protons. The following quantities will be used in the discussion of the results:

- Q^2: The photon virtuality, i.e. the absolute value of the squared 4-momentum transfer at the electron (the generic term 'electron' is used for both e^+ and e^-) vertex. In the results presented here Q^2 ranges from ~ 0 to ~ 80 GeV^2.

- $W_{\gamma p}$: the CM energy of the $\gamma^* p$ system, here in the range $20 \lesssim W_{\gamma p} \lesssim 285$ GeV.

- t: The squared 4-momentum transfer at the proton vertex, with $0 \lesssim |t| \lesssim 10$ GeV^2 in the present results. For small values of Q^2, $|t|$ is well approximated by the squared transverse momentum of the produced vector meson V, $t \approx -p_t^2$.

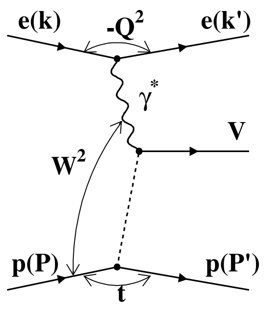

Figure 1: Schematic diagram of elastic vector meson production in ep scattering.

The γ^* energies available at HERA make it possible, within a single experiment, to study the process of exclusive vector meson production over a large $W_{\gamma p}$ interval and with a very wide range of the scales: Q^2, t and M_V, where M_V is the mass of the vector meson V.

The detectors of the H1 and ZEUS experiments are both all-purpose detectors, excellently suited for detection and reconstruction of the vector meson decays, for measuring the Q^2 and t values of the reactions, and for distinguishing the pure elastic processes from those where the proton dissociates. Also in such p-dissociative reactions the few-body decay products of the vector meson are clearly separated, by several units of rapidity, from the low-mass multi-particle system resulting from the proton dissociation.

The following presentation is structured into a photoproduction section, where results in which Q^2 is small are discussed, and an electroproduction section, in which Q^2 takes larger values. In each of these regimes results will be presented for both low and high V masses. In the last section photoproduction results, in which the variable $|t|$ takes on large values, are presented.

2 Photoproduction

Fig. 2 shows a compilation of the cross section measurements $\sigma_{\gamma p \to Vp}$ vs. $W_{\gamma p}$, for exclusive photoproduction of vector mesons at HERA and at lower (fixed target) CM energies. Also the total photoproduction cross section is shown. The measurements show one of the typical features of soft diffractive processes, namely the slow rise of the cross section with $W_{\gamma p}$, for $W_{\gamma p} \gtrsim 10$ GeV. Soft diffractive processes are well described within the framework of Regge phenomenology and the Vector Meson Dominance (VMD) model. In this approach the exclusive vector meson production at high energies is assumed to proceed via the exchange of a Pomeron trajectory; the $W_{\gamma p}$ and t dependences of the cross section are coupled:

$$\frac{\mathrm{d}\sigma_{\gamma p}}{\mathrm{d}|t|} \propto e^{-b_0|t|} \left(\frac{W_{\gamma p}^2}{W_0^2} \right)^{2(\alpha(t)-1)} \quad (1)$$

Here $\alpha(t) = \alpha(0) + \alpha' t$; the constants b_0 and W_0 are process dependent.

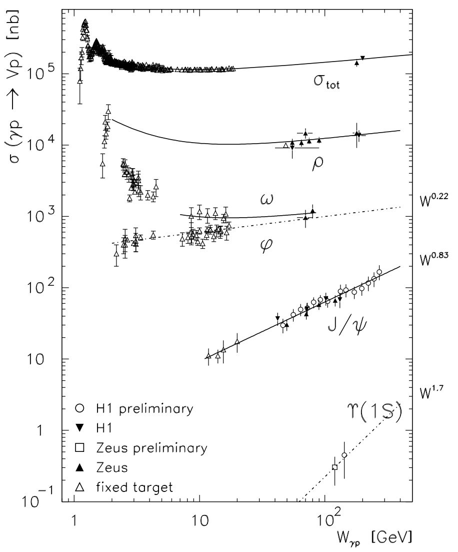

Figure 2: Compilation of $\sigma_{\gamma p}^{tot}$ and $\sigma_{\gamma p}$ for exclusive photoproduction of the vector mesons $\rho^\circ, \omega, \phi, J/\Psi$ and Υ, vs. $W_{\gamma p}$. Full curves represent fits using Regge parametrizations and assuming single pomeron exchange. The dashed lines indicate $W_{\gamma p}$ dependences as written at the right hand side.

The slope b of the t distribution is then $b = b_0 + 2\alpha' \ln(W_{\gamma p}^2/W_0^2)$. After integration over t, the effective power of a $W_{\gamma p}^\delta$ dependence of the cross section is $\delta \simeq 4(\alpha(0) - 1 - \alpha'/b)$. Fits[1] to hadron-hadron scattering and photoproduction data give $\alpha(0) = 1.08$ and $\alpha' = 0.25$ GeV^{-2}. For the light vector mesons slope values of typically $b \simeq 10$ GeV^{-2} are found. As can be seen in Fig. 2, the predicted δ values of ~ 0.22 are in good agreement with the measurements for the light vector mesons ρ°, ω and ϕ.

No such agreement is seen for the photoproduction of heavy vector mesons. The increase of the cross section of J/Ψ is much steeper than the soft prediction, with a power $\delta \approx 0.8$. Moreover, the measured slope of the t dis-

tribution for J/Ψ production is smaller than for the light vector mesons, $b_{J/\Psi} \simeq 5$ GeV^{-2}, giving the expectation $\delta \simeq 0.14$.
The exclusive J/Ψ photoproduction data, including brand new data from H1[2], are shown again in Fig.3 together with two different theoretical approaches.

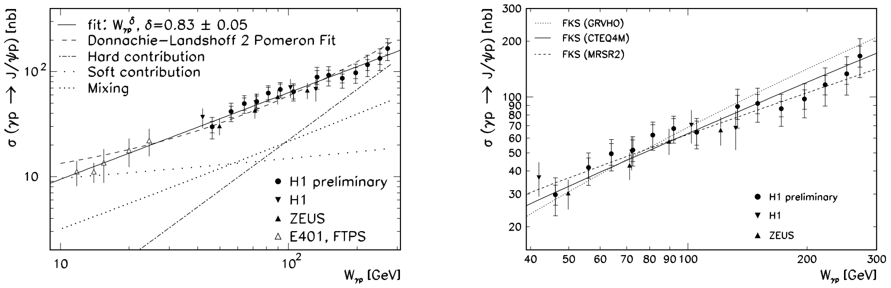

Figure 3: Total elastic J/ψ cross section $\sigma_{\gamma p}$ as a function of $W_{\gamma p}$ compared to different models.

The Regge approach: In an effort to save the approach within the framework of Regge phenomenology, Donnachie and Landshoff[3,4] added a second, "hard" pomeron trajectory to the exchange. Fig.3 shows that a fit with 2 pomerons indeed provides a reasonable description of the data. A good theoretical motivation for the "hard" pomeron is however lacking, although the authors discuss the possibility of glueball exchange.

The pQCD approach: The presence of a hard scale, provided through the heavy c quark mass, suggests an approach within perturbative QCD. Motivated by the very different time scales involved, factorization is assumed (and later proven) in such models, i.e. the $\gamma^* p \to Vp$ scattering is viewed as a sequence of events[5] well separated in time. This is illustrated in Fig.4. The steps are:

- The virtual photon fluctuates into a $q\bar{q}$ pair.
- The $q\bar{q}$ pair scatters off the proton.
- The scattered $q\bar{q}$ pair forms a bound state.

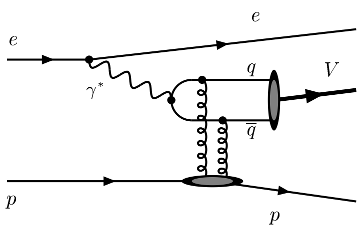

Figure 4: Schematic diagram of elastic vector meson production in ep scattering, via t-channel exchange of a gluon pair.

In leading order the scattering of the $q\bar{q}$ pair off the proton is mediated by the t-channel exchange of two gluons, in a colour singlet state. The cross section becomes proportional to the square of the gluon density $g(x, Q^2)$ in the proton,

$$\sigma \propto \alpha_s^2(Q^2)/Q^6 \; [xg(x, Q^2)]^2, \tag{2}$$

where x is the Bjorken x. Fits of the model of Frankfurt, Koepf and Strikman[6] (FKS) are shown in Fig.3, for several parameterisations of the gluon density in the proton. It is seen that the cross section is very sensitive to the gluon density parameterisation; while the CTEQ4M and MRSR2 parametrisations can describe the data, the GRVHO parameterisation has a tendency which is steeper than the data.
The steep rise of the $\gamma p \to J/\Psi p$ cross section with $W_{\gamma p}$ has a simple explanation in the pQCD models: it is a consequence of the increasing gluon density of the proton at small x. Using Ryskin's[7] proposed scale $\mu^2 = (Q^2 + M_{J/\Psi}^2 + |t|)/4$ for photoproduction at small $|t|$, a value $\mu^2 = 2.4$ GeV^2 is obtained. At this scale, and at small x, the gluon density rises[8] as $xg(x) \propto x^{-0.2}$. Using the approximate relation $xW_{\gamma p}^2 \approx Q^2$, valid at small x and at fixed Q^2, one finds that $\sigma_{\gamma p \to J/\Psi p} \propto W_{\gamma p}^{0.8}$, in good agreement with the observation.

Shrinkage: The logarithmic $W_{\gamma p}$ dependence of the elastic slope parameter b, known as shrinkage, is a prediction of the soft pomeron model, and has been observed for the light vector mesons. pQCD, in which there is no coupled $W_{\gamma p}$ and t dependence, in contrast predicts no shrinkage of the diffractive peak. It is therefore interesting to determine the value of α' in J/Ψ photoproduction. The new H1 data have been used also to this effect.

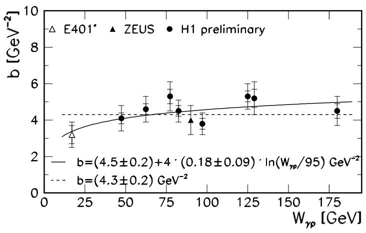

Figure 5: Slope b vs. $W_{\gamma p}$.

Fig.5 shows the slope parameter b, obtained in 5 different $W_{\gamma p}$ bins, together with data from ZEUS and from the fixed target experiment E401[9]. Fits with and without (i.e. α' set to 0) the logarithmic $W_{\gamma p}$ dependence indicate that shrinkage cannot be excluded; the effect is however only 2 s.d., with $\alpha' = 0.18 \pm 0.09$ GeV^{-2}.

A more direct determination of the Regge trajectory has been made by Levy[10] and by H1. In their analysis, H1 determined $\alpha(t) = \alpha(0) + \alpha' t$ in 5 bins of t, fitting in each t-bin i the $W_{\gamma p}$ dependence of eq.(1). Fig. 6 shows the result of the linear fit of the resulting 5 values of $\alpha(t_i)$, with the central value and its

1 s.d. band. Again no clear conclusion can be drawn, the data are compatible both with no shrinkage and with the presence of shrinkage, weaker than in the soft pomeron model.

Fig. 6 also shows the trajectories expected for the soft and hard pomeron (for the latter $\alpha' = 0.1$ GeV^{-2} is estimated[4]); the H1 measurement lies between these predictions. The BFKL (Balitsky, Fadin, Kuraev, Lipatov) pomeron[11] trajectory is in rough agreement with the measurement (the value $\alpha' = 0$ was assumed by H1, since only the intercept is predicted).

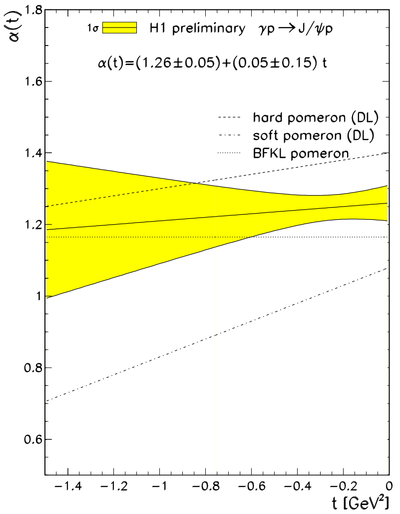

Figure 6: The measured Regge trajectory $\alpha(t) = \alpha(0) + \alpha' t$ for elastic J/Ψ photoproduction.

Elastic photoproduction of Υ: The cross section measurements[12,13] of Υ photoproduction are shown in Fig. 7. The published ZEUS measurement, based on the $\mu^+\mu^-$ decay of Υ, has now been combined with a new, preliminary measurement based on detection in the e^+e^- decay channel[14]. A number of theoretical predictions of the cross section as function of $W_{\gamma p}$ are also shown in Fig. 7. The early prediction by Frankfurt, Koepf and Strikman[6] is about 2 s.d. too low. The measurements of H1 and ZEUS have inspired recent improvements of theory. Taking into account the fact that at large vector meson masses the off-diagonal gluon distributions in the exchange are important, and including also the real part of the amplitude, Frankfurt, McDermott and Strikman[15] (FSM), and Martin, Ryskin and Teubner[16] (MRT), can now give a good description of the measurements. The importance of including the real part of the amplitude in the calculations is shown by the 2 curves labelled FSM and FSM(only Im).

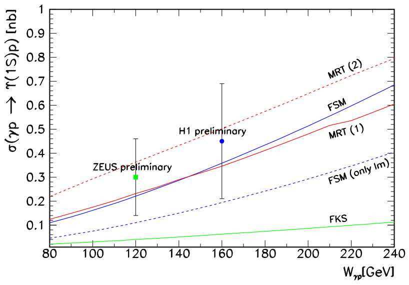

Figure 7: Υ photoproduction cross section vs. $W_{\gamma p}$, together with theoretical predictions.

3 Electroproduction

Elastic electroproduction of vector mesons at HERA offers new rich possibilities for tests of QCD, since here the scale Q^2 can be varied over a large range. Not only can the Q^2 dependence of the cross section be studied and compared to that of eq.(2), but the measurement of the Q^2 dependence of other observables will provide insight into the transition from the soft, non-perturbative to the hard, perturbative regime. In particular the light vector meson electroproduction is of great interest. New, high statistics data from H1 and ZEUS on the electroproction of ρ° [17,18], ω [19], ϕ [20] and J/Ψ [17,21] are described in the following.

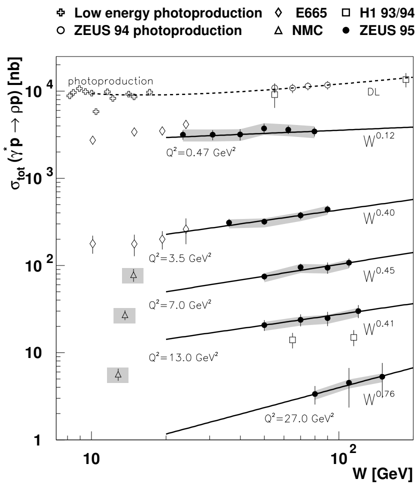

Figure 7: Cross section for electroproduction of ρ°, vs. $W_{\gamma p}$. Error bands are indicated. The curves represent fits of the dependence $\sigma \sim W_{\gamma p}^{\delta}$

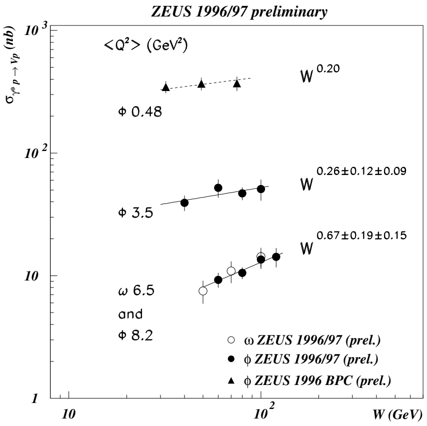

Figure 8: Cross sections for electroproduction of ω and ϕ, as function of $W_{\gamma p}$. Solid curves show fits to the ϕ cross section. The dotted line shows the $W_{\gamma p}^{0.20}$ dependence for comparison.

$W_{\gamma p}$ dependence: The new ZEUS cross section measurements of elastic ρ°, ϕ and ω electroproduction are presented in Figs. 7 and 8, as function of $W_{\gamma p}$ and for several values of the average Q^2. The cross sections rise with increasing $W_{\gamma p}$, and the higher the average Q^2, the faster is the rise. This observation can be quantified with fits to the form $W_{\gamma p}^{\delta}$ in each Q^2 bin. As already discussed, the parameter δ is in Regge phenomenology related to the exchange trajectory, $\delta \simeq 4(\alpha(\langle t \rangle) - 1)$, with $\alpha(t) = \alpha(0) + \alpha' t$. Using $\langle t \rangle = 1/b$

(see below) and $\alpha' = 0.25\ \mathrm{GeV}^{-2}$, H1 obtained with their new ρ° electroproduction data the Q^2 dependence of the intercept $\alpha(0)$, Fig.9. The data suggest that with increasing Q^2 the intercept of the effective trajectory governing ρ° electroproduction is larger than 1.08, the "soft pomeron" intercept.

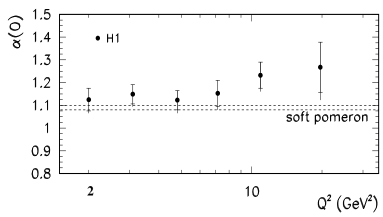

Figure 9: Q^2 dependence of the intercept $\alpha(0)$ for elastic ρ° production. The dashed lines represent the range of values obtained for the "soft pomeron" intercept[3,22].

Q^2 dependence of $\sigma(\gamma^* p \to Vp)$: The cross section eq.(2) contains the factor $1/Q^6$, characteristic for "soft" diffraction. In pQCD this steep Q^2 dependence is however modified by the Q^2 dependence of α_s and of the gluon density. The steepness of the Q^2 dependence of the cross section is also modified by e.g. the Fermi motion of the quarks[5,23], which suggests that, beyond the pQCD tests, precise measurements of the Q^2 dependence of the cross section for elastic vector meson electroproduction can reveal information also about the wave functions of the vector mesons.

Fig.10 shows the Q^2 dependence of the H1 and ZEUS data on exclusive elastic ρ° and ϕ electroproduction, at $\langle W_{\gamma p}\rangle$ values of 75 and 80 GeV, respectively. The curves show fits of the form $(Q^2 + M_\rho^2)^{-n}$ (ρ°) and $(Q^2)^{-n}$ (ϕ). The values obtained, $n = 2.24 \pm 0.09$ and $n = 2.18 \pm 0.10(stat.) \pm 0.15(syst.)$ respectively, confirm the less steep Q^2 dependence expected from pQCD. Similar agreement with the form $(Q^2 + M_\omega^2)^{-2}$ is obtained for the ω electroproduction data (not shown). Note that in the case of the ϕ data the fit includes only data points at $Q^2 \geq 5\ \mathrm{GeV}^2$, and the dashed curve extrapolates the fit to lower Q^2 values. Here the exclusion of the M_ϕ^2 term lets the fit lie far above the data.

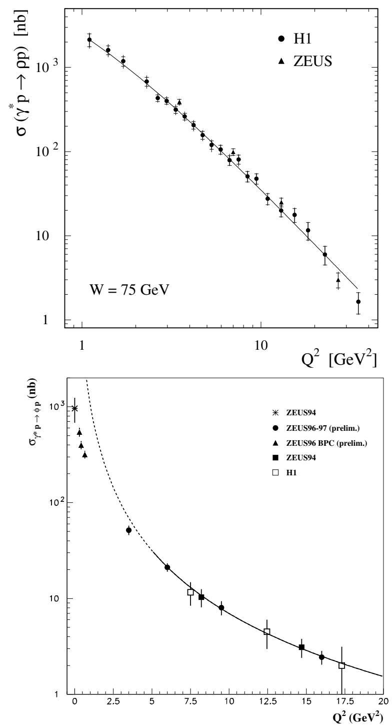

Figure 10: ρ° and ϕ electroproduction cross sections vs. Q^2. The curves are explained in the text.

In Fig.11 the Q^2 dependence of the $\sigma(\gamma^* p \to \rho^\circ p)$ data is directly compared to several model calculations: The Generalized VMD model (GVDM) of Schildknecht, Schuler and Surrow[24] falls above the data at larger Q^2 values, while the pQCD inspired model of Cudell and Royen[25] gives a good description of the data, down to the photoproduction measurements. The model of Martin, Ryskin and Teubner[26], also pQCD inspired, cannot describe the data.
It is interesting to note that the Q^2 dependence of the cross section is also reasonably described in a Regge-eikonal approach, reported by Prokudin elsewhere in these proceedings[27].

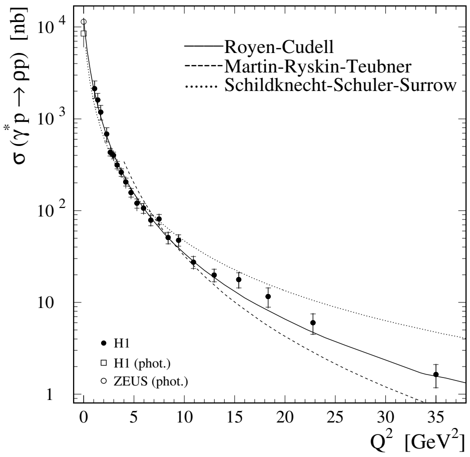

Figure 11: Elastic ρ° electroproduction cross section vs. Q^2, compared to pQCD and GVDM models.

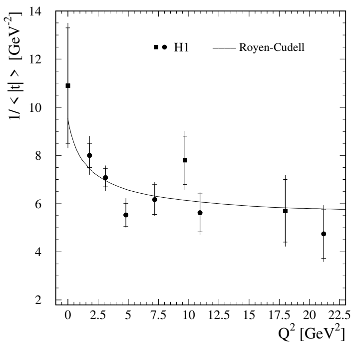

Figure 12: Q^2 dependence of the slope parameter b for elastic ρ° electroproduction, compared to a pQCD model and presented in the form of the variable $1/\langle|t|\rangle$.

Q^2 dependence of the slope parameter b: It was already mentioned in the previous discussion that the slope parameter b of the diffractive peak is considerably smaller (~ 5 GeV^{-2}) in elastic J/Ψ photoproduction, compared to the values found (~ 10 GeV^{-2}) for the light vector mesons. This can be interpreted as a reflection of the smaller transverse size of the virtual photon, fluctuating into a $q\bar{q}$ system, when the quark mass scale is increased. It is then interesting to see if increasing another scale, Q^2, leads to a similar decrease of the slope parameter b. Fig.12 shows the H1 results for the Q^2 dependence of the parameter b in elastic ρ° production, plotted here in the form of the variable $1/\langle|t|\rangle$ (identical to b for an exponential t distribution). A strong

decrease is indeed seen, going from the photoproduction point to higher Q^2 values. Relating b to the radii of the scattering particles, $b \propto R_p^2 \oplus R_{q\bar{q}}^2$, and remembering that $R_p^2 \sim 4-5$ GeV^{-2}, one can conclude that with increasing Q^2 the $q\bar{q}$ system becomes small compared to the proton and that it therefore starts to probe the structure of the proton.
Fig.12 also shows a comparison of the data with the model of Cudell and Royen[25]. Good agreement is seen.
At the lowest Q^2 values (Beam Pipe Calorimeter, BPC data) ZEUS find evidence for shrinkage of the diffractive peak in the elastic ρ° electroproduction data, while at larger Q^2 values no conclusive results are obtained.

$W_{\gamma p}$ dependence of $\sigma(\gamma^* p \to J/\Psi p)$: Fig.13 shows the $W_{\gamma p}$ dependence of the cross section for elastic J/Ψ electroproduction, for several values of Q^2. New data from H1 and ZEUS provide these results. As was already discussed in the previous photoproduction section, the c quark mass provides a hard scale, so that with increasing Q^2 now two hard scales come into play. The dash-dotted curves in Fig.13, which show fits of the form $W_{\gamma p}^{\delta}$, demonstrate that adding a new hard scale does not change the behaviour of the $W_{\gamma p}$ dependence of the cross section. The steep rise of the cross section, which was observed already in the J/Ψ photoproduction data, stays practically the same at larger values of Q^2.
The data are compared to the model calculations (full and dashed curves)

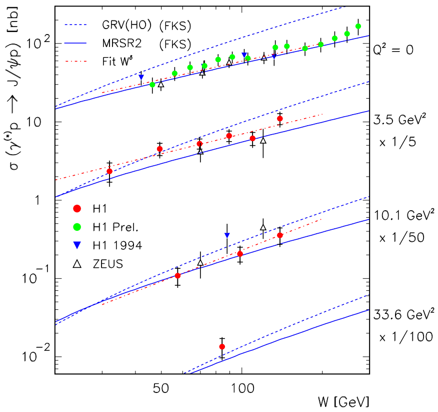

Figure 13: J/Ψ elastic electroproduction cross section vs. $W_{\gamma p}$ for several values of Q^2. The curves are explained in the text.

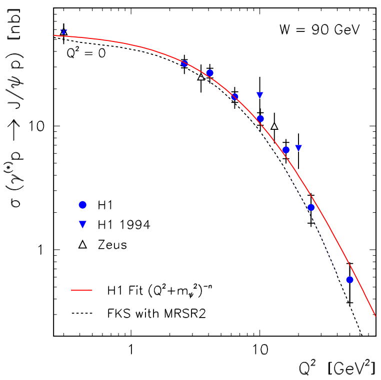

Figure 14: Q^2 dependence of elastic J/Ψ electroproduction. The curves are explained in the text.

of Frankfurt, Koepf and Strikman[6], using two different parameterisations of the proton gluon density. Data are precise enough to allow some distinction of the parameterisations.

Q^2 dependence of $\sigma(\gamma^* p \to J/\Psi p)$: The Q^2 dependence of elastic J/Ψ production is shown in Fig.14. The data have been fitted (full curve) to the form $(Q^2 + M^2_{J\Psi})^{-n}$, with $n = 2.38 \pm 0.11$ as result. The dotted curve shows the Frankfurt, Koepf and Strikman model calculation, using the MRSR2 proton gluon parameterisation.
It is worthwhile to note that the value of the power n, 2.38, is close to the values found for similar fits to the Q^2 dependence of the low mass vector meson cross sections. A compilation of all HERA data on $\sigma(\gamma^* p \to Vp)$, using a universal scale $(Q^2 + M_V)/4$, has recently been presented and discussed[28].

Q^2 dependence of the slope b in J/Ψ electroproduction: H1 have used their elastic J/Ψ electroproduction data to determine the diffractive slope parameter b in 2 bins of Q^2, namely $2-8$ GeV^2 and $8-80$ GeV^2. The results, $b = 4.4 \pm 0.4 \pm 0.4$ and $b = 2.5 \pm 0.6 \pm 0.6$ GeV^{-2}, respectively, give a weak indication that b decreases with increasing Q^2. $b = 5.1 \pm 1.3$ GeV^{-2} for $2 < Q^2 < 40$ GeV^2 is found by ZEUS. The low Q^2 results for both experiments are compatible with the photoproduction values for the slope parameter b. None of the experiments find any significant dependence on $W_{\gamma p}$ for b.

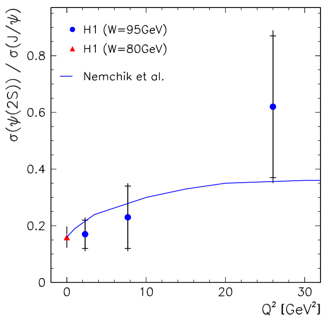

Figure 15: Ratio of the cross sections for quasi-elastic production of $\Psi(2S)$ and J/Ψ, vs. Q^2. The curve shows the calculation of Nemchik et al.[29].

Q^2 dependence of Ψ' electroproduction: H1 has recently also presented data on electroproduction of $\Psi(2S)$, using the decay $\Psi' \to J/\Psi \pi^+\pi^-, J/\Psi \to e^+e^-, \mu^+\mu^-$. The scarce data ("quasi-elastic", i.e. including both elastic and low-mass proton dissociative events) have been divided into 3 Q^2 bins and are shown in Fig.15, in the form of the ratio $\sigma(\gamma^* p \to \Psi(2S)p)/\sigma(\gamma^* p \to J/\Psi p)$ vs. Q^2. The data at low Q^2 values agree with the previous photoproduction measurement. There is an indication that the cross section ratio rises with increasing Q^2, which is also predicted in pQCD models[6,29]. An asymptotic value of 0.5 is predicted in[6]. The curve in Fig.15 shows the model calculation of Nemchik et al.[29], based on colour dipole phenomenology.

Flavour independence at large Q^2 values: At sufficiently high scale values one expects that the vector meson production process becomes independent of the participating quark flavour. Simple counting of the quark charges, together with the assumption of a point-like electromagnetic coupling to the quark charges, give the ratios, well known from SU(4), of $9:1:2:8$ for the ρ°, ω, ϕ and J/Ψ vector mesons. It is also well known that at low energies this expectation is not fulfilled by the cross section ratios $\sigma_{\gamma^* p \to Vp}/\sigma_{\gamma^* p \to \rho^\circ p}$, with $V = \phi, \omega$ and J/Ψ. Figs.16 and 17 show the HERA results for these cross section ratios as function of Q^2, with the limits expected from SU(4) indicated as dashed lines. For the light vector mesons good agreement is seen between the cross section ratios and the expectation; in the case of ω already for small Q^2, in the case of ϕ for Q^2 values $\gtrsim 8$ GeV^2. In the case of the J/Ψ meson, the data in Fig.17 indicate that the limit is reached only at still larger Q^2 values.

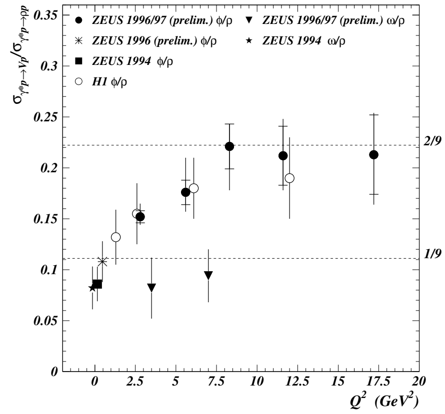

Figure 16: Cross section ratios $\sigma_{\gamma^* p \to Vp}/\sigma_{\gamma^* p \to \rho^\circ p}$ vs. Q^2, with $V = \phi$ and ω. The $SU(4)$ predictions are indicated by dashed lines.

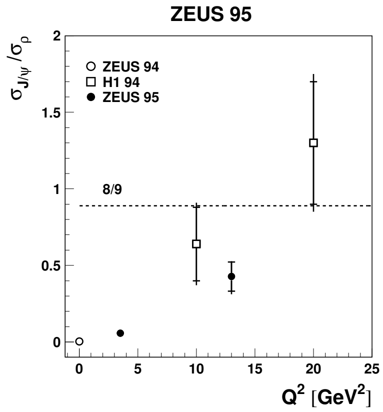

Figure 17: Cross section ratio $\sigma_{\gamma^* p \to J\Psi p}/\sigma_{\gamma^* p \to \rho^\circ p}$ vs. Q^2. The dashed line shows the SU(4) prediction.

Helicity Studies: The study of the angular distributions of the production and decay of the vector mesons V in the reaction $\gamma^* p \to Vp$ provides information about the polarization states of the photon and the vector mesons V. Such studies are particularly interesting at large values of Q^2, since many theoretical models make firm predictions about the polarization in this regime. Thus pQCD models predict dominance at high Q^2 of longitudinally polarized vector mesons from longitudinally polarized photons.
In their studies, which are so far limited to 2-body decays of vector mesons, H1 and ZEUS define three angles in the helicity system, the commonly used reference frame, as shown for $V = \rho^\circ$ in Fig.18. The angles are:

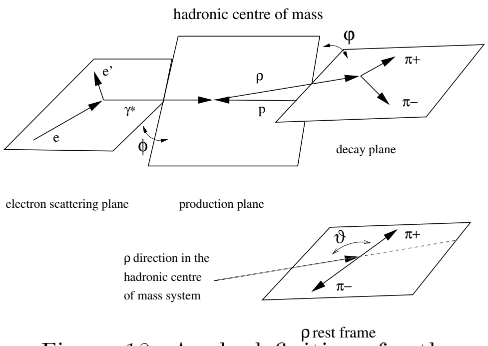

Figure 18: Angle definitions for the helicity system in elastic vector meson production.

- ϕ: in the hadronic (γp) CM the azimuthal angle between the electron scattering plane and the plane containing V and the scattered proton,
- θ: the decay angle of the 2-body decay of V, defined by the positive decay particle in the rest system of V, with the quantization axis taken as the direction of V in the γp CM,
- φ: the azimuthal angle of the positive decay particle in the rest system of V.

The normalized angular distribution $W(\cos\theta, \varphi, \phi)$ can be written[30] as a function of 15 quantities $r^\alpha_{ik}, r^{04}_{ik}$, which are linear combinations of the spin density matrix elements ρ^α_{ik},

$$r^{04}_{ik} = \frac{\rho^0_{ik} + \epsilon R \rho^4 ik}{1 + \epsilon R} \qquad r^\alpha_{ik} = \frac{\rho^\alpha_{ik}}{1+\epsilon R},\ \alpha = 1,2 \qquad r^\alpha_{ik} = \frac{\sqrt{R}\rho^\alpha_{ik}}{1+\epsilon R},\ \alpha = 5,6$$

Here ϵ is the polarization parameter of the virtual photon, being ≈ 0.99 in the present analyses. $R = \sigma_L/\sigma_T$ is the ratio of the longitudinal and transverse $\gamma^* p$ cross sections. The ρ^α_{ik} elements depend on bilinear combinations of the helicity amplitudes and the subscripts i and k take the values of the possible helicity states $-1, 0, 1$. The superscripts 0 and 4 refer respectively to unpolarized transverse photons and longitudinally polarized photons, superscripts 1 and 2 correspond to linearly polarized transverse photons, and superscripts 5 and 6 represent the interference of transverse and longitudinal amplitudes.

In the case of S-channel helicity conservation (SCHC) and natural parity exchange (NPE) the 15 independent density matrix elements ρ_{ik}^{α} are constrained, and only 5 elements are non-zero.

H1 and ZEUS have performed large statistics helicity analyses of elastic ρ° [18,31] and ϕ [20] electroproduction. The result for the ρ° analysis is shown for the two experiments in Fig.19, where all 15 quantities r_{ik}^{α}, r_{ik}^{04} have been determined. One notes the very good agreement between the two experiments. The prediction from SCHC and NPE is also shown as a dotted curve. The data agree with this prediction, except for the quantity r_{00}^{5}, which is clearly non-zero where the SCHC prediction is zero. The pQCD model of Ivanov and Kirschner[32], which takes into consideration the momentum distribution of the vector meson quark constituents, in contrast predicts this violation of SCHC, and is in excellent agreement with the data. Recent calculations of Royen and Nikolaev[33] also reproduce the observed SCHC violation.

In their analysis of the ϕ data (not shown) ZEUS obtained a similar, although statistically less significant, result.

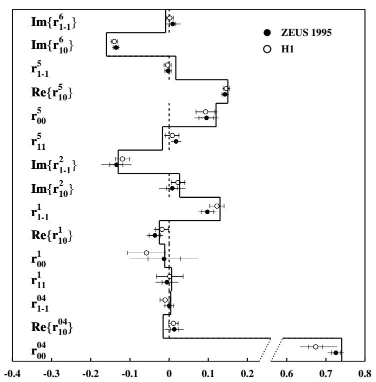

Figure 19: The 15 combinations $r_{ik}^{04}, r_{ik}^{\alpha}$ of the spin density matrix elements, obtained in the ρ° analysis. The curves are explained in the text.

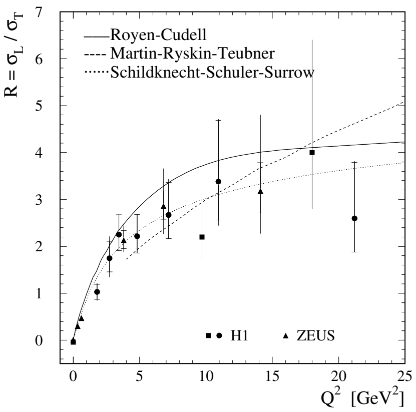

Figure 20: Ratio R of the longitudinal to transverse cross sections for elastic ρ electroproduction, vs. Q^2. The curves represent predictions from models based on pQCD and GVDM.

The element r_{00}^{5} is approximately proportional to the amplitude T_{01} for a transverse photon to produce a longitudinal vector meson. H1 have estimated the size of the T_{01} amplitude relative to the non-flip amplitudes, finding that the effect is 8 ± 3 %. This is in rough agreement with similar results, obtained at lower energy in fixed target experiments[34].

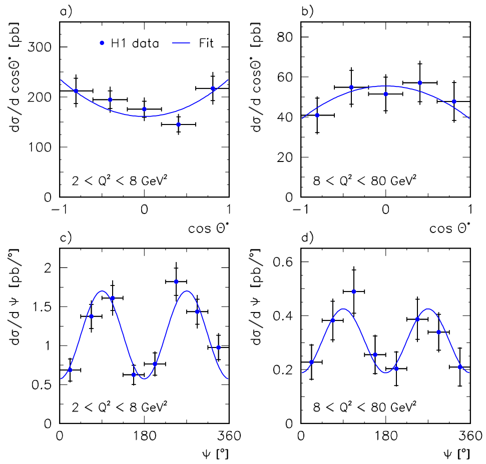

Figure 21: Angular distributions for the positive lepton in J/Ψ decays, obtained in quasi-elastic $\gamma^* p$ production of J/Ψ in 2 bins of Q^2 and for $40 < W_{\gamma p} < 160$ GeV. The curves are explained in the text.

The SCHC violation effect being small, one can further explore the angular dependence under the assumption of validity of SCHC and NPE. One prediction is then the relation $r^1_{1-1} = 1/2\,(1 - r^{04}_{00})$, valid independent of the value of the ratio R. The measurements are in agreement with this relation within 1 s.d., thereby providing an independent check of the assumption. Furthermore, if SCHC is valid for the interaction, then the ratio R can be directly obtained, via the relation

$$R = \frac{\sigma_L}{\sigma_T} = \frac{1}{\epsilon}\,\frac{r^{04}_{00}}{1 - r^{04}_{00}}.$$

r^{04}_{00} is the probability to produce longitudinally polarized vector mesons, from either transversely or longitudinally polarized photons. The R values measured under this assumption (the influence of the SCHC violating effect on R results in a 2-3 % overestimate) are shown in Fig.20, as function of Q^2. A steep increase of R is observed when Q^2 increases from the photoproduction point (R is expected to be 0 for $Q^2 = 0$), while R seems to flatten out at larger Q^2 values. A clear dominance of the longitudinal cross section is observed already at Q^2 values of a few GeV^2. The data are in good agreement with previous fixed target measurements (not shown). The magnitude of the ratio, as well as its Q^2 dependence, are well reproduced by model calculations, some of which are shown in Fig.20. This is true both for the pQCD inspired models[25,26] and for the GVDM model[24].

The value of R has been determined also for J/Ψ production, in data where also low-mass proton dissociative states are included. The statistics do not allow a full angular analysis as in the ρ° and ϕ cases. Instead, 1-dimensional distributions of $\cos\theta$ and $\Psi = \varphi - \phi$ are used to extract the spin density matrix element combinations r^{04}_{00} and r^{1}_{1-1}:

$$\frac{d\sigma}{d\cos\theta} \propto 1 + r^{04}_{00} + (1 - 3r^{04}_{00})\cos^2\theta, \qquad \frac{d\sigma}{d\Psi} \propto 1 - \epsilon r^{1}_{1-1}\cos 2\Psi.$$

The H1 data and the fits to these distributions are shown in Fig.21.

The extracted values for r^{1}_{1-1} and r^{04}_{00} are found to satisfy the relation $r^{1}_{1-1} = 1/2\,(1 - r^{04}_{00})$ within 1 s.d., thus giving support for the assumption of SCHC and NPE validity in the J/Ψ production process.

$< Q^2 >$ (GeV^2)	R	exp.
0	0.17 ± 0.14	H1
0	-0.01 ± 0.09	ZEUS
4	$0.18^{+0.18}_{-0.14}$	H1
5.9	$0.41^{+0.45}_{-0.52}$	ZEUS
16	$0.94^{+0.79}_{-0.43}$	H1

Table 1: Values for the ratio R in J/Ψ production.

The values for the ratio R, shown in Table 1, suggest that R increases with increasing Q^2, in particular when taking the earlier photoproduction results[35,36] into account.
The values of R obtained here are much smaller than the ones determined for elastic ρ and ϕ production at similar Q^2. However, when considering the measurements on the global scale Q^2/M_V^2, they are of the same order.

4 Photoproduction of vector mesons at large $|t|$

New data have been presented by ZEUS[19], for photoproduction of the vector mesons ρ°, ϕ and J/Ψ at large values of $|t|$, from 1 up to 11 GeV^2. While in the case of the scale Q^2 the vector meson p_t is balanced by the momentum transfer to the electron, it is here balanced by the momentum transfer to the proton. The question addressed is thus whether also $|t|$, like Q^2, can serve as a hard scale in perturbative QCD descriptions of the processes, and if so, at which values of $|t|$ the calculations become reliable.
At large values of $|t|$ the exclusive vector meson production process is dominated by low-mass proton dissociative events and detector components close to the proton beamline can be used to distinguish these from the elastic events. The scattered electron was tagged by a calorimeter close to the electron beamline, so that $Q^2 < 0.01$ GeV^2 and $80 < W_{\gamma p} < 120$ GeV. Two of these new ZEUS results are discussed here.

Helicity studies of ρ° production: The spin density matrix element combinations r^{04}_{00}, Re$[r^{04}_{10}]$ and r^{04}_{1-1} are shown vs. $|t|$ in Fig.22.

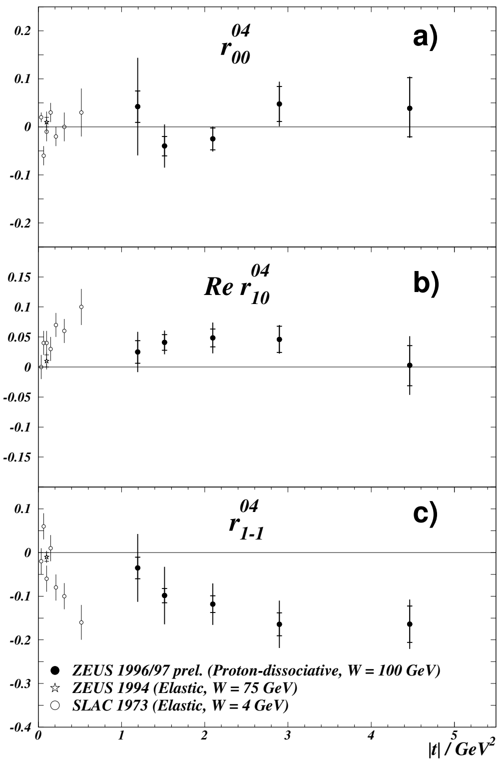

Figure 22: The spin-density matrix element combinations r^{04}_{00}, Re$[r^{04}_{10}]$ and r^{04}_{1-1}, vs. $|t|$. ZEUS photoproduction data $\gamma p \to VN$, with N being a proton or a low-mass dissociated state.

Ivanov and Ginzburg[37] and Brodsky et al.[38] predict that at large values of $|t|$ the production of longitudinally polarized ρ° will dominate. Since r^{04}_{00} is the probability to obtained longitudinal ρ°, it is thus expected to be large at large values of $|t|$. As seen in Fig.22, data up to $|t|$ values of 4-5 GeV^2 do not support this prediction, r^{04}_{00} is compatible with being zero everywhere. One can conclude that the perturbative regime with $|t|$ as a scale is not yet reached.

The quantity Re$[r^{04}_{10}]$, which corresponds to an interference between the helicity conserving amplitude and the single flip amplitude, is non-zero at higher $|t|$ values and thus indicates evidence for a single flip contribution in the production process.

The quantity r^{04}_{1-1} is significantly non-zero at larger values of $|t|$. This indicates that a double flip contribution becomes important, i.e. a transversely polarized photon produces a ρ° with the opposite helicity. This is a violation of SCHC.

The latter results confirm previous fixed target measurements at SLAC[39], also shown in Fig.22. However, the results are still preliminary. One uncertainty is a possible non-resonant di-pion background under the ρ°.

Flavour independence limit: As already discussed in the case of the scale Q^2, one expects in pQCD the interaction to be flavour independent at large enough values of the scale. ZEUS have used their data at high $|t|$ to test this prediction also in the case when the scale is provided by the momentum transfer at the proton vertex. Fig.23 shows ratios of the cross sections for ϕ and J/Ψ production, relative to the cross section for ρ°, vs $|t|$. The expected limits from a pointlike electromagnetic interaction with the quarks forming the vector mesons are indicated with dotted lines. It is seen that the ϕ data are consistent with this expectation over the whole $|t|$ range, while the J/Ψ data are significantly lower than the limit, for $|t|$ values below $\sim$ 4 GeV^2.

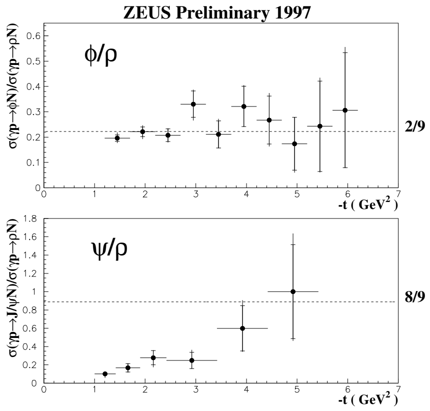

Figure 23: Cross section ratios $\sigma(\gamma^* p \to VX)/\sigma(\gamma^* p \to \rho^\circ X)$ vs. $|t|$, with V being J/Ψ or ϕ, and X being a proton or a proton dissociative system. ZEUS preliminary data. The dotted lines are explained in the text.

5 Conclusions

The years of high luminosity running at HERA have opened up a rich field of precise data on exclusive vector meson production, spanning large intervals of $W_{\gamma p}$, Q^2, M_V and $|t|$. This new wealth of data extends the results obtained in the earlier fixed target experiments. Whereas these early results could be successfully interpreted in a "soft", VMD-Regge approach, the new HERA data open up access to larger values of several scales, thereby entering the realm of validity of perturbative QCD. Thus the data span the very interesting region of transition between "soft" and "hard" diffractive interactions. While there is good evidence in the present data that both Q^2, M_V and $|t|$ all serve successfully as hard scales in perturbative QCD calculations for diffractive reactions, this field of research remains very active. Further fruitful interaction between theory and experiments will certainly provide new and interesting knowledge, not only about the structure of the proton and the vector mesons, but also about the complex nature of the diffractive interactions.

Acknowledgments

It is a pleasure to thank the organizers for the warm and agreeable atmosphere in a most interesting and well prepared conference. I also wish to thank all my colleagues in H1 and ZEUS, for providing the data shown in this report and for all their help given to me.

References

1. A. Donnachie and P.V. Landshoff, Phys. Lett. **B296** (1992) 227
2. H1 Collab., C. Adloff et al., contr. paper 157aj to EPS-HEP 1999, Tampere, Finland
3. A. Donnachie and P.V. Landshoff, Phys. Lett. **B348** (1995) 213
4. A. Donnachie and P.V. Landshoff, Phys. Lett. **B437** (1998) 408
5. S.J. Brodsky et al., Phys. Rev. **D50** (1994) 3134;
J.C. Collins, L. Frankfurt and M. Strikman, Phys. Rev. **D56** (1997) 2982
6. L. Frankfurt, W. Koepf and M. Strikman, Phys. Rev. **D57** (1998) 512
7. M.G. Ryskin, Z. Phys. **C57** (1993) 89
8. M. Erdmann, in Proceedings of the 29th Intern. Conference on High Energy Physics, Vancouver 1998, Editors A. Astbury, D. Axen and J. Robinson, Vol. 1, p. 217
9. E401 Collab., M. Binkley et al., Phys. Rev. Lett. **48** (1982) 73
10. A. Levy, Phys. Lett. **B424** (1998) 191
11. S.J. Brodsky et al., hep-ph/9901229 (1999)
12. ZEUS Collab., J. Breitweg et al., Phys. Lett. **B437** (1998) 432
13. H1 Collab., C. Adloff et al., contr. paper 574 to ICHEP 1998, Vancouver
14. P. Merkel, to be published in the proceedings, EPS-HEP 1999, Tampere, Finland
15. L. Frankfurt, M.F. McDermott and M. Strikman, JHEP **9902** (1999) 2
16. A.D. Martin, M.G. Ryskin and T. Teubner, Phys. Lett. **B454** (1999) 339
17. ZEUS Collab., J. Breitweg et al., Eur. Phys. J. **C6** (1999) 603
18. H1 Collab., C. Adloff et al., DESY-99-010, to appear in Eur. Phys. J. C
19. ZEUS Collab., contr. paper 499 to EPS-HEP 1999, Tampere, Finland
20. ZEUS Collab., contr. paper 793 to ICHEP 1998, Vancouver
21. H1 Collab., C. Adloff et al., Eur.Phys.J. **C10** (1999) 373
22. J.R. Cudell, K. Kang and S. Kim, Phys. Lett. **B395** (1997) 311
23. L. Frankfurt, W. Koepf and M. Strikman, Phys. Rev. **D54** (1996) 3194
24. D. Schildknecht, G.A. Schuler and B. Surrow, Phys. Lett. **B449** (1999) 328

25. J.R. Cudell and I. Royen, Phys. Lett. **B545** (1999) 505
26. A.D. Martin, M.G. Ryskin and T. Teubner, Phys. Rev. **D55** (1997) 4329
27. V.A. Petrov and A.V. Prokudin, these proceedings and hep-ph/9912245(1999)
28. B. Clerbaux, hep-ph/9908519
29. J. Nemchik et al., Phys. Lett. **B258** (1991) 493;
    J. Nemchik et al., J. Exp. Theor. PHys. **86** (1998) 1054
30. K. Schilling and G. Wolf, Nucl. Phys. **B61** (1973) 381;
    for a detailed discussion, see also J.A. Crittenden, Springer Tracts in Modern Physics, Volume 140 (Springer, Berlin Heidelberg, 1997)
31. ZEUS Collab., J. Breitweg et al., DESY-99-102, to appear in Eur. Phys. J. C
32. D.Yu.Ivanov and R. Kirschner, Phys. Rev. **D58** (1998) 114026
33. I. Royen, N. Nikolaev, to be published in the proceedings, 7th Intern. Conference on Deep Inelastic Scattering and QCD, 19-23 April, 1999, Zeuthen, Germany
34. P. Joos et al., Nucl. Phys. **B113** (1976) 53;
    CHIO Collab., W.D. Shambroom et al., Phys. Rev. **D25** (1982) 1
35. H1 Collab., S. Aid et al., Nucl. Phys. **B472** (1996) 3
36. ZEUS Collab., M. Derrick et al., Phys. Lett. **B377** (1996) 259
37. D. Yu. Ivanov, Phys. Rev. **D53** (1996) 3564;
    I.F. Ginzburg and D.Yu. Ivanov, Phys. Rev. **D54** (1996) 5523
38. S.J. Brodsky et al., Phys. Lett. **B449** (1999) 306
39. J. Ballam et al., Phys. Rev. **D7** (1973) 3150